Am J Physiol Endocrinol Metab 290: E870–E881, 2006.
First published December 13, 2005; doi:10.1152/ajpendo.00233.2005.

Cardiac metabolism in mice: tracer method developments and in vivo application revealing profound metabolic inflexibility in diabetes

Nicholas D. Oakes,[1] Pia Thalén,[1] Ellen Aasum,[2] Amanda Edgley,[1] Terje Larsen,[2] Stuart M. Furler,[3] Bengt Ljung,[1] and David Severson[4]

[1]*AstraZeneca R&D, Mölndal, Sweden;* [2]*University of Tromsø, Tromsø, Norway;* [3]*Garvan Institute, Sydney, Australia; and* [4]*University of Calgary, Calgary, Alberta, Canada*

Submitted 25 May 2005; accepted in final form 6 December 2005

Oakes, Nicholas D., Pia Thalén, Ellen Aasum, Amanda Edgley, Terje Larsen, Stuart M. Furler, Bengt Ljung, and David Severson. Cardiac metabolism in mice: tracer method developments and in vivo application revealing profound metabolic inflexibility in diabetes. *Am J Physiol Endocrinol Metab* 290: E870–E881, 2006. First published December 13, 2005; doi:10.1152/ajpendo.00233.2005.— Studies of cardiac fuel metabolism in mice have been almost exclusively conducted ex vivo. The major aim of this study was to assess in vivo plasma FFA and glucose utilization by the hearts of healthy control (*db/+*) and diabetic (*db/db*) mice, based on cardiac uptake of (R)-2-[9,10-^{3}H]bromopalmitate ([^{3}H]R-BrP) and 2-deoxy-D-[U-^{14}C]glucose tracers. To obtain quantitative information about the evaluation of cardiac FFA utilization with [^{3}H]R-BrP, simultaneous comparisons of [^{3}H]R-BrP and [^{14}C]palmitate ([^{14}C]P) uptake were first made in isolated perfused working hearts from *db/+* mice. It was found that [^{3}H]R-BrP uptake was closely correlated with [^{14}C]P oxidation ($r^2 = 0.94$, $P < 0.001$). Then, methods for in vivo application of [^{3}H]R-BrP and [^{14}C]2-DG previously developed for application in the rat were specially adapted for use in the mouse. The method yields indexes of cardiac FFA utilization (R_f*) and clearance (K_f*), as well as glucose utilization (R_g'). Finally, in the main part of the study, the ability of the heart to switch between FFA and glucose fuels (metabolic flexibility) was investigated by studying anesthetized, 8-h-fasted control and *db/db* mice in either the basal state or during glucose infusion. In control mice, glucose infusion raised plasma levels of glucose and insulin, raised R_g' (+58%), and lowered plasma FFA level (−48%), K_f^* (−45%), and R_f^* (−70%). This apparent reciprocal regulation of glucose and FFA utilization by control hearts illustrates metabolic flexibility for substrate use. By contrast, in the *db/db* mice, glucose infusion raised glucose levels with no apparent influence on cardiac FFA or glucose utilization. In conclusion, tracer methodology for assessing in vivo tissue-specific plasma FFA and glucose utilization has been adapted for use in mice and reveals a profound loss of metabolic flexibility in the diabetic *db/db* heart, suggesting a fixed level of FFA oxidation in fasted and glucose-infused states.

fatty acid; glucose; metabolic flexibility; bromopalmitate tracer; deoxyglucose tracer

THE HEART CAN METABOLIZE exogenous substrates such as glucose and free fatty acids (FFA) to provide ATP. FFA is generally considered to be the preferred myocardial substrate, with FFA oxidation accounting for 60–70% of cardiac energy metabolism (32, 48).

Diabetes results in enhanced cardiac disease due to *1*) increased coronary heart disease (accelerated atherogenesis) and *2*) a cardiomyopathy, defined as ventricular dysfunction in the absence of detectable coronary heart disease or hypertension (13, 38). Because rodents are resistant to atherosclerosis, any cardiac dysfunction observed with a rodent model of diabetes will reflect diabetic cardiomyopathy.

Diabetic *db/db* mice provide a monogenic model of obesity and insulin resistance, characteristics of type 2 diabetes (10, 26). Perfused *db/db* hearts, studied ex vivo, exhibit features of a diabetic cardiomyopathy, with reduced cardiac contractile function and altered myocardial metabolism (38). An elevated rate of FFA oxidation is the earliest metabolic change evident in hearts from 6-wk *db/db* mice, preceding any change in glucose oxidation or contractile function (1). At 12 wk of age (at an established stage of diabetes), *db/db* hearts are characterized as having increased FFA oxidation together with decreased glucose utilization, reduced contractile performance, and increased susceptibility to ischemic damage (1, 3).

The metabolic alterations in diabetic hearts may have functional implications in terms of contractile performance (38), an example of a metabolic maladaptation (45, 51). For example, the overutilization of FFA by *db/db* hearts with intracellular lipid accumulation (7) could cause contractile dysfunction as a consequence of lipotoxicity (39). In support of this hypothesis, normalization of glucose and FFA metabolism in hearts from transgenic *db/db* mice overexpressing the insulin-regulatable glucose transporter (GLUT4) was associated with complete normalization of cardiac contractile function (3).

However, it must be acknowledged that the experimental evidence for enhanced cardiac FFA utilization in diabetic mice has come exclusively from ex vivo studies with perfusions containing only two substrates, glucose and an FFA (usually palmitate) present at typical (nondiabetic) concentrations. Thus it is reasonable to anticipate that the metabolic phenotype of a diabetic heart might be altered markedly by elevated concentrations of glucose and FFA that correspond to hyperglycemic and hyperlipidemic conditions in vivo. In addition, a number of other substrates in vivo are available for myocardial utilization. For example, both lactate and pyruvate can make important contributions to total carbohydrate oxidation by perfused hearts (27). Furthermore, the utilization of ketone bodies by diabetic hearts could suppress FFA oxidation (21). Finally, insulin present in vivo at elevated concentrations (hyperinsulinemia) in *db/db* mice could also influence myocardial metabolism, depending on the degree of cardiac insulin sensitivity. Metabolic flexibility refers to the ability of an organ and organism to shift substrate utilization as part of homeostatic adaptability

Address for reprint requests and other correspondence: N. Oakes, Integrative Pharmacology, AstraZeneca R&D, S-431 83 Mölndal, Sweden (e-mail: nick.oakes@astrazeneca.com).

The costs of publication of this article were defrayed in part by the payment of page charges. The article must therefore be hereby marked "*advertisement*" in accordance with 18 U.S.C. Section 1734 solely to indicate this fact.

(44). For example, metabolically healthy hearts have a well-developed capacity to switch between lipid and carbohydrate fuels, depending on insulin levels and substrate availability in the circulation. Therefore, it is essential to investigate FFA metabolism in vivo to assess metabolic flexibility and to substantiate the conclusion from ex vivo perfusions that FFA utilization is enhanced in diabetic hearts (7).

FFA metabolism can be studied in vivo on the basis of the principle of metabolic trapping by use of infusions of trace amounts of (R)-2-[^{3}H]bromopalmitate ([^{3}H]R-BrP), a partially metabolized FFA analog, and [^{14}C]palmitate ([^{14}C]P) (33, 34). However, these tracer methods have not been optimized for use in the mouse. Moreover, the detailed quantitative relationship between [^{3}H]R-BrP and native FFA uptake by the heart is unknown. Such information may be obtained from an experimental system in which [^{3}H]R-BrP utilization can be studied simultaneously with native FFA traced with radiolabeled palmitate ([^{14}C]P). Therefore, the objectives of the present investigation were *1*) to assess quantitatively the metabolism of [^{3}H]R-BrP and [^{14}C]P simultaneously, using ex vivo perfused hearts from control mice; *2*) adapt the in vivo tracer method developed in the rat (33, 34) to mice to assess cardiac metabolism; and *3*) compare in vivo FFA and glucose metabolism by control (*db/+*) and diabetic (*db/db*) hearts, with particular attention to the assessment of metabolic flexibility in the diabetic hearts.

METHODS AND MATERIALS

General Overview

First, ex vivo experiments were performed to examine the quantitative nature of the relationship between [^{3}H]R-BrP and native FFA ([^{14}C]P) uptake and metabolism by the mouse heart. For this purpose, an isolated working heart system was employed. Conditions were varied by pharmacological and physiological means between individual ex vivo heart perfusion experiments to produce a range in FFA metabolism over which to compare the analog and native tracers. Then, two separate in vivo studies were performed after adaptation of methods to the very small size of the mouse. In vivo *study 1* assessed cardiac FFA metabolism in a group of metabolically normal control mice by use of the combination of [^{3}H]R-BrP and [^{14}C]P tracers. Analogous to the ex vivo experiments, conditions were varied across individual animals by pharmacological and physiological means with the aim of producing a wide range in cardiac FFA oxidation rates. For in vivo *study 2*, [^{3}H]R-BrP was applied in combination with 2-deoxy-D-[U-^{14}C]glucose ([^{14}C]2-DG) to study cardiac FFA and glucose metabolism in control and *db/db* mice. To assess metabolic flexibility, animals were studied in either the basal fasting state or during an intravenous glucose infusion.

Ex Vivo Study of Perfused Hearts from Control Mice: Assessment of Cardiac FFA Metabolism with [^{3}H]R-BrP

Animals. Male control C57BL/KsJ (*db/+*) mice (15–17 wk) were purchased from Harlan (UK). The animals were housed in a room with controlled temperature (20–22°C) and relative humidity (40–60%) with a 12:12-h light-dark cycle. Mice had free access to tap water and standard rodent chow.

Perfused working heart preparation. Hearts from control male (*db/+*) mice were perfused essentially according to procedures detailed in Ref. 4. Briefly, after cannulation of the aorta (using an 18-gauge plastic cannula), the left atrium was cannulated with a 16-gauge steel cannula. Tracer studies were performed in spontaneously beating hearts in working mode, with a filling pressure (preload) of 12.5 mmHg and the left ventricle ejecting against an afterload of 55 mmHg. Hearts were perfused in a recirculating system (total volume 35 ml) with a modified Krebs-Henseleit bicarbonate buffer (37°C, gassed with 5% CO_2-95% O_2, pH 7.4; for ionic composition see Ref. 4) with either 5 or 11 mM glucose, as well as 0.6 mM palmitate bound to 3% bovine serum albumin (BSA, fraction V, A-8022; Sigma). The heart and buffer system is enclosed in an airtight apparatus with an injection port providing access to the perfusion buffer for withdrawal of samples or tracer delivery. Gases exit the system only by bubbling through a hyamine hydroxide (1 M) solution, which quantitatively traps all of the contained CO_2. Cardiac function was monitored by measuring aortic flow and coronary flow as well as heart rate, as previously described (4).

Perfusion conditions for individual experiments. Perfusion conditions were varied across individual experiments to generate a range in cardiac FFA metabolism for correlations between [^{3}H]R-BrP and [^{14}C]P uptake and metabolism (Table 1). Compared with standard conditions (here defined as condition Norm), a low buffer glucose concentration (LoGlu) and increased mechanical work (LoGluHiWork), achieved by modest increases in preload (from 12.5 to 17.5 mmHg) and afterload (from 55 to 75 mmHg), were used with the intention of elevating FFA oxidation. By contrast, two concentrations of insulin in the buffer (LoIns and HiIns) were employed with the intention of suppressing FFA oxidation and stimulating acylglyceride synthesis. One additional perfusion experiment (PoorFunct) was performed opportunistically using a heart with markedly impaired function, with coronary flow and cardiac output ~30% of the other perfused hearts.

Preparation of tracer. Organic solvent stock solutions of [^{3}H]R-BrP and [^{14}C]P were evaporated to dryness (N_2, room temperature) in a glass test tube, unlabeled perfusate was added to the tube, and the solution was gently mixed and warmed over a period of ≥1 h. By use of this method, ~60% of the radioactivity dried onto the glass surface of the test tube is recovered into bulk solution in the perfusate.

Tracer experiment. Immediately before tracer administration, baseline samples of buffer and the hyamine hydroxide CO_2 trap were collected. The tracer experiment commenced with injection of 2.5 ml of perfusate, containing ~10 ×10^6 dpm [^{3}H]R-BrP and ~5 ×10^6 dpm [^{14}C]P, into the apparatus injection port. After 10–11 min, samples of the buffer (2.5 ml) and the CO_2 trap (2 × 0.35 ml) were collected. The heart was then quickly switched to a tracer-free buffer solution for 30 s (to rinse out tracer contained within the cardiac vasculature), removed from the apparatus, and frozen in liquid N_2-cooled tongs. The buffer samples were used for determination of [^{14}C]P and [^{3}H]R-BrP concentration, as well as [^{14}C]bicarbonate (see *Sample Analysis*). Samples of the hyamine CO_2 trap solution were analyzed for [^{14}C]bicarbonate content (described below). The heart was analyzed for total ^{3}H and ^{14}C content, and a lipid analysis was performed to quantify [^{14}C]palmitate and its incorporation into the major lipid classes, as well as the (nonmetabolized) [^{3}H]R-BrP content (see below).

Table 1. *Conditions utilized for individual perfusion experiments*

Condition	*n*	Glucose, mM	FFA, mM	Insulin, nM	CO·P, ml·mmHg·min^{-1}
LoGluHiWork	1	5	0.6	0	1,350
LoGlu	2	5	0.6	0	1,020
Norm	2	11	0.6	0	1,000
LoIns	2	11	0.6	1.8	940
HiIns	2	11	0.6	6.0	830
PoorFunct	1	5	0.6	0	340

Perfusate concentrations of glucose, free fatty acids (FFA), and insulin. *n* = number of hearts studied under each condition. The LoGluHiWork heart was perfused with a preload of 17.5 mmHg and an afterload of 75 mmHg. All other perfusions were performed with a preload of 12.5 mmHg and an afterload of 55 mmHg. Cardiac function/work was assessed on the basis of the product of cardiac output and estimated peak systolic pressure (CO·P).

Sample Analysis

Determination of buffer [^{3}H]R-BrP and [^{14}C]P concentrations. Tracer concentrations in buffer samples (50 μl) were determined as described below.

DETERMINATION OF BUFFER [^{14}C]BICARBONATE CONTENT. The majority of the $^{14}CO_2$ produced by oxidation of [^{14}C]palmitate and then released from the heart exists in the form of [^{14}C]bicarbonate dissolved in the perfusate. Perfusate samples (0.75 ml) were analyzed for [^{14}C]bicarbonate concentration using methods detailed previously (4).

DETERMINATION OF $^{14}CO_2$ IN THE HYAMINE CO_2 TRAP. Some of the $^{14}CO_2$ produced by oxidation of [^{14}C]palmitate leaves the perfusate via breakdown of [^{14}C]bicarbonate; the resulting $^{14}CO_2$ is then captured in the hyamine hydroxide trap. Samples (0.35 ml) of this solution were pipetted directly into liquid scintillation vials for counting.

CARDIAC ^{14}C AND ^{3}H CONTENT AND LIPID CLASS DISTRIBUTION. One ~25-mg piece of the frozen heart was used to determine total ^{14}C and ^{3}H content by use of complete tissue oxidation (described below). A second piece of the heart (~50 mg) was used for lipid extraction and class separation (described below).

In Vivo Studies

Animals. Experimental procedures were approved by the Local Ethics Review Committee on Animal Experiments (Göteborg Region). Male BKS.Cg-m-Lepr^{db}/Lepr^{db} diabetic (*db/db*) and nondiabetic heterozygous controls (*db/+*) were purchased from Taconic Europe (Ry, Denmark) and housed for ≥1 wk before study in a room with controlled temperature (20–22°C) and relative humidity (40–60%) with a 12:12-h light-dark cycle. The mice had free access to tap water and standard rodent chow (R3; Lactamin, Stockholm, Sweden) and were 11–13 wk old at the time of study.

Animal preparation: method development. Methodology originally developed for the rat (34) had to be modified for the much smaller size of a mouse. In particular, derivation of useful flux information from the tracers is dependent on a means of accurately quantifying the area under the arterial plasma tracer curves (AUCs) over the 10- or 12-min experimental protocols (see below) while minimizing cardiovascular disturbances due to blood sampling. The method previously employed in the rat (34), requiring multiple and frequent blood samples at discrete time points, was not considered optimal for use in the mouse. Instead, an approach based on a constant, slow withdrawal of arterial blood (6 μl/min) from the carotid catheter was used. Preliminary experiments showed little if any impact of this blood withdrawal on heart rate or blood pressure if the withdrawal was matched by simultaneous infusion of 4% BSA in saline. The plasma tracer levels in the resulting single blood sample pooled over the 10- or 12-min periods are the true time-averaged levels, which can be used to directly calculate the AUCs (see *Calculations*). To enable the constant withdrawal of blood without influencing plasma FFA levels, whole body anticoagulation therapy was achieved using a direct-acting thrombin inhibitor (melagatran, AstraZeneca R&D, Mölndal, Sweden), administered intravenously as a bolus 3 min before commencement of the tracer infusion. We verified that this procedure has no influence on systemic blood pressure, heart rate, or plasma FFA concentration in the anesthetized mouse.

The durations of the tracer experiments, 10 min for the [^{3}H]R-BrP/[^{14}C]P combination (in vivo *study 1*) and 12 min for the [^{3}H]R-BrP/[^{14}C]2-DG combination (in vivo *study 2*), were chosen on the basis of preliminary studies of [^{3}H]R-BrP, [^{14}C]P, and [^{14}C]2-DG plasma kinetics. Plasma tracer time course data following intravenous administration was obtained using a variant of the constant withdrawal method described above (Fig. 1). Briefly, arterial blood was withdrawn at a constant rate into a length of PE50 tubing. Blood withdrawn over each minute was separated from the previously withdrawn

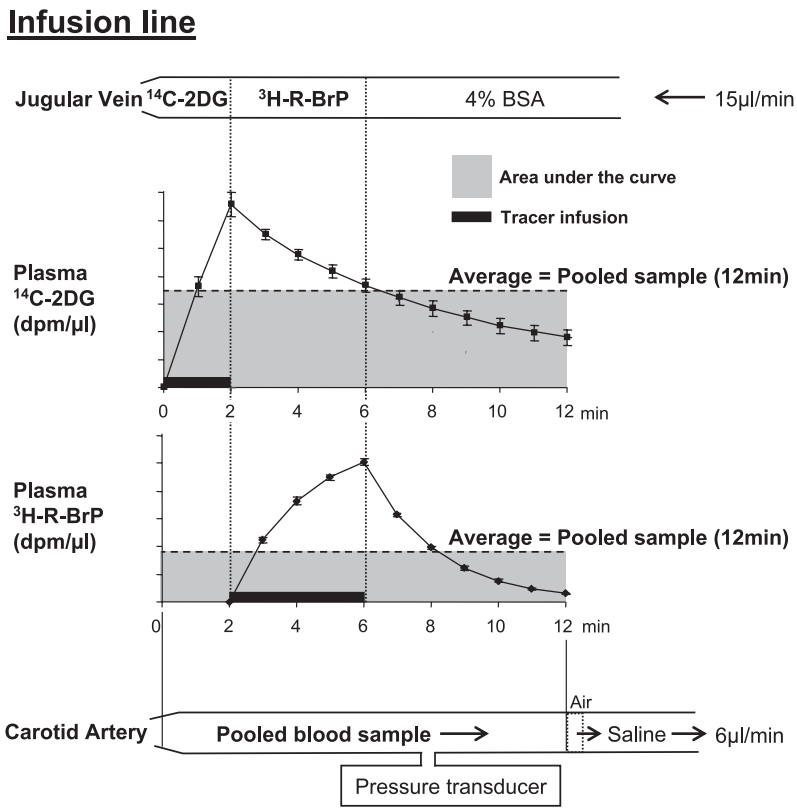

Fig. 1. Tracer methodology in the mouse. The 2 tracers, 2-deoxy-D-[U-^{14}C]glucose ([^{14}C]2-DG) and (R)-2-[9,10-^{3}H]bromopalmitate ([^{3}H]R-BrP), are arranged in series in the jugular infusion line (*top*) before the tracer experiment. Sequential delivery of the tracers, first [^{14}C]2-DG (0–2 min) and then [^{3}H]R-BrP (2–6 min), after tracer infusion start generates the in vivo plasma tracer profiles drawn. These profiles plot actual data obtained in pilot experiments in C57BL/6 mice. In vivo areas under the plasma tracer curves, needed for calculation of plasma glucose and FFA fluxes into the heart, were obtained from a single pooled sample (*bottom*) continuously withdrawn throughout the 12-min experiment. Plasma tracer concentrations in this pooled sample were equal to time-averaged plasma levels (indicated by horizontal dashed lines).

blood by introducing a small air bubble into the PE50 tubing, from an air-filled microsyringe via a T-connection, at the beginning of each minute. Plug flow, due to the presence of the air bubbles in the tubing, prevented the individual segments from mixing. At the end of the experiment, blood in each minute's segment was transferred into a small capillary tube and centrifuged, and the plasma was separated and analyzed for tracer content. On the basis of the data obtained in these preliminary experiments (Fig. 1), disappearance of the infused tracers from the plasma into the tissues by the time of heart collection at the end of the experiments should be >80% for [^{14}C]2-DG and >95% for [^{3}H]R-BrP and [^{14}C]P.

Surgical preparation and catheter implantation. Mice were anesthetized with intraperitoneally administered Na-thiobutabarbitol (Inactin; RBI, Natick, MA); control and *db/db* mice received 150 μg/g (3 μl/g) and 225 μg/g (4.5 μl/g), respectively. Immediately after induction of anesthesia, mice were placed on a warmed table to prevent an otherwise rapid drop in body temperature. A 1.2-mm-diameter thermocouple probe was inserted 2.5 cm into the rectum for body temperature measurement, which was used to control a heating lamp to hold body temperature at 37°C. To maintain a free airway, a tracheotomy was performed just below the level of the larynx, and a 3-cm length of PE90 tubing (Becton-Dickinson, Stockholm, Sweden) was inserted ~5 mm into the trachea.

The left carotid artery and right jugular vein were catheterized with PE10 tubing. The carotid catheter was connected to a pressure transducer (model DPT-6100; Smiths Medical Sverige, Sollentuna, Sweden) and maintained patent with a continuous infusion of a sterile saline solution containing sodium citrate (20.6 mM, 3 μl/min). Mean arterial pressure, heart rate, and rectal temperature were monitored and stored in a computer-based custom-made system.

To ensure a stable anesthetic depth, the barbiturate anesthesia was supplemented during the experiment with inhalation of isoflurane (Forene; Abbott Scandinavia, Solna, Sweden). This was achieved by passing an isoflurane-in-O_2 stream over the tracheal cannula opening. Anesthetic depth was monitored by periodically testing for the presence of foot withdrawal, bradycardia, and blood pressure lowering in response to foot pinching. Anesthetic delivery was set to the minimal concentration of isoflurane required to abolish these reflexes (usually 2.0–2.5% at steady state). The concentration of isoflurane, which has minimal cardiodepressive influence (28), was adjusted using an anesthesia unit (Univentor 400; AgnTho's, Lidingö, Sweden).

Tracer Experiments

Preparation for tracer infusion and blood sampling. Approximately 90 min after completion of surgery, an intravenous bolus of the thrombin inhibitor melagatran (3 nmol/g, 1 μl/g) was administered. A catheter line was connected to the jugular cannula having the following serially arranged components (Fig. 1): a glass syringe in an infusion pump filled with 4% BSA in sterile normal saline, an air bubble, ~150 μl of 4% BSA in sterile normal saline, and then tracer solution(s) in normal saline. The air bubble traveled steadily through the infusion line, thereby minimizing mixing of the serially arranged components but never reaching the jugular vein due to the length of the catheter. For withdrawal of the arterial blood sample, a 50-cm length of PE50 catheter, connected at one end to a glass syringe in a reversible syringe pump (CMA 1100; Carnegie Medicin, Solna, Sweden), was filled with melagatran in normal saline (100 μM) and wound around an aluminum cylinder that was then placed in ice. The end of this catheter was connected to the carotid catheter via a T-junction. The other arm of the T-junction was connected to the pressure transducer. Just before commencement of tracer infusion and blood sample withdrawal, an air bubble was introduced via the pressure transducer arm into the sampling catheter just outside the carotid artery to minimize mixing of the withdrawn blood and subsequent dilution with saline.

Tracer infusion and blood and tissue sampling. The tracer experiment began at ~14:30, ~1.5 h after completion of surgery. Tracer infusion into the jugular vein (15 μl/min) and blood sample withdrawal from the carotid artery (6 μl/min) were commenced simultaneously. Infusion of 15 μl/min tracer-free 4% BSA in sterile saline into the jugular vein continued until the end of the experiment. At either 10 min (in vivo *study 1*) or 12 min (in vivo *study 2*), withdrawal of the pooled arterial blood sample was stopped, the withdrawal line was disconnected, and ~200 μl arterial blood were collected for clinical chemistry analyses. The heart was quickly removed for weighing and measurement of tracer retention (see *Analysis of Plasma and Tissue Samples*). The pooled blood sample contained in ice-chilled PE50 tubing was carefully transferred to an EDTA tube, centrifuged, and used to obtain the time-averaged plasma tracer concentrations. For this purpose, a 10-μl plasma aliquot was placed directly into 2 ml of lipid extraction mixture (described below) and stored at −20°C for later analysis.

Glucose Infusion

In some animals (see below), a constant intravenous glucose infusion of 2.2 μmol/min (2 μl/min 20% glucose) was commenced ~45 min before commencement of the tracer experiment. The rate of glucose delivery was intended to be of physiological magnitude, sufficient to promote insulin secretion, and was comparable in magnitude to reported steady-state glucose infusion rates required to maintain euglycemia in anesthetized normal mice in response to hyperinsulinemia (16, 30, 37).

In Vivo Study 1: Estimation of In Vivo Cardiac FFA Oxidation in Control Mice

Study conditions. Conditions were varied among individual control mice with the aim of creating a range of cardiac FFA oxidation from low to high rates: two mice were studied during an intravenous glucose infusion (Glucose), as described above; one was studied in the fed state (Fed) and two following a 7-h fast (Fasted); two mice were studied during inotropic/chronotropic stimulation (Dobutamine), achieved using an intravenous infusion of dobutamine (16 $\mu g \cdot kg^{-1} \cdot min^{-1}$, Dobutrex; Eli Lilly, Stockholm, Sweden).

Tracer. The tracer solution containing albumin-bound [^{3}H]R-BrP and [^{14}C]P was freshly prepared on each experiment day. Ethanol (5 μl) containing ~8×10^6 dpm [^{3}H]R-BrP, 7×10^6 dpm [^{14}C]P, and 60 nmol Na-palmitate (Sigma, St. Louis, MO) was added to 120 μl of 4% essentially fatty acid-free bovine serum albumin (BSA; Sigma) in sterile saline. Each mouse was infused with 60 μl of tracer solution containing ~4×10^6 dpm [^{3}H]R-BrP (equivalent to 33 pmol/mouse) and 3.5×10^6 dpm [^{14}C]P.

Protocol. The tracer solution, containing [^{3}H]R-BrP and [^{14}C]P, was infused over a period of 0–4 min. Blood sample withdrawal started at 0 min and stopped at 10 min, at which time a final blood sample was collected (for plasma glucose, insulin, and FFA determinations), and immediately after that the heart as well as other tissues were dissected for analysis (see below).

In Vivo Study 2: Cardiac Metabolism in Diabetic and Nondiabetic Mice

Groups. Four groups of 8-h-fasted mice were studied: two basal groups, *db/db* fasted and control fasted, and two groups that were studied during an intravenous glucose infusion, *db/db*-glucose and control-glucose.

Tracers. Saline solution was prepared containing [^{14}C]2-DG (Amersham, Solna, Sweden) at ~150×10^6 dpm/ml and stored in aliquots at −20°C until the experiment day. A separate tracer solution containing albumin-bound [^{3}H]R-BrP was prepared, essentially following the in vivo *study 1* method for tracer preparation (above) but excluding [^{14}C]P. Each mouse was infused with ~4.5×10^6 dpm [^{14}C]2-DG and 4.0×10^6 dpm [^{3}H]R-BrP.

Protocol. Figure 1 depicts the setup for the tracer experiment. Note the serially arranged [^{3}H]R-BrP and [^{14}C]2-DG tracers in the jugular line. Plasma kinetics (determined in separate studies in C57Bl/6JolaHsd mice) are illustrated, showing initial entry of the infused [^{14}C]2-DG (0–2 min) followed by entry of the much more rapidly cleared [^{3}H]R-BrP (over 2–6 min). Blood sample withdrawal ended at 12 min. A large blood sample (~200 μl) was collected for plasma glucose, insulin, triglyceride (TG), FFA, ketone body, and blood gas analyses. The heart was quickly dissected for analysis (see below).

Synthesis, Resolution, and Identification of Optical Enantiomers of [9,10-^{3}H]-2-Bromopalmitate

Racemic (R,S)-2-[9,10-^{3}H]bromopalmitic acid was synthesized from [9,10-^{3}H]palmitic acid (1.96 TBq/mmol; Amersham) by a Hell-Volhard-Zelinsky reaction (20), as previously described (34). The pure (R)- and (S)-enantiomers were obtained by chromatographic resolution on a Chiralpak AD column (Chiral Technologies Europe, Illkirch Cedex, France) with 2% 2-propanol and 0.1% formic acid in acetonitrile (2). The Chiralpak AD column shows high selectivity and resolution for the stereoisomers of [^{3}H]R-BrP and allows much higher loadability of the racemate (mg/injection) onto the column than the method reported earlier (34). Radiochemical detection was used for collection. Assignment of absolute configurations of the separated (R)- and (S)-enantiomers was accomplished by an enantioselective lipase-catalyzed esterification of racemic 2-[9,10-^{3}H]bromopalmitic acid with *n*-butanol in hexane (24). After 65% conversion, the acid fraction was isolated, and HPLC analysis showed only one peak coinciding with the slower eluting enantiomer from the chiral column. The enantiomeric purity of the (R)-isomer was determined to be >99% e.e. with an optical rotation of +25.7° (1% in $CHCl_3$, $[\alpha]_D^{25}$). The (+)-enantiomer has previously been assigned to have the R-configuration (22). The radiochemical purity of ^{3}H-labeled material used to prepare the infusate (described below) was >95% [^{3}H]R-BrP, as determined by HPLC.

Analysis of Plasma and Tissue Samples

Plasma lipids, glucose, lactate, β-butyrate (β-HBA), and insulin. Colorimetric kit methods were used for the measurement of plasma FFA (NEFA C; Wako, Richmond, VA), TG (Triglycerides/GB; Boehringer Mannheim, Indianapolis, IN), glucose (Glucose HK; Roche, Stockholm, Sweden), D-3-hydroxybutyrate (RANBUT; Randox, Antrim, UK), and lactate [L-lactate (PAP), Randox]. Spectrophotometric analysis was performed using a Cobas Mira analyzer (Hoffman-La Roche, Basle, Switzerland). Insulin concentrations were measured using radioimmunoassay (rat insulin RIA kit; Linco Research, St. Charles, MO).

Resolution of buffer/plasma [^{3}H]R-BrP, [^{14}C]P, and [^{14}C]2-DG. A lipid extraction procedure based on the method in Ref. 17 was performed on buffer/plasma samples. Plasma (10 μl) or buffer (50 μl) was pipetted into 2 ml of the mixture isopropanol-isohexane-1 M acetic acid (40:10:1). Briefly, addition of 1.2 ml of 1 M acetic acid and 1.2 ml of isohexane results in phase separation and partitioning of [^{14}C]2-DG, if present, into the lower aqueous phase. From the upper phase, polar lipids including [^{3}H]R-BrP and [^{14}C]P (if present) were separated from neutral lipids by means of solid-phase extraction (200-mg NH_2 columns, Isolute; Sorbent, Göteborg, Sweden).

Cardiac ^{3}H and ^{14}C content and lipid class distribution. For determination of total cardiac ^{3}H and ^{14}C content, a piece of heart tissue was weighed and placed in a small cardboard cone for combustion. Total tissue ^{3}H and ^{14}C activities were determined using a Packard System 387 Automated Sample Preparation Unit (Packard Instrument, Meriden, CT), which completely oxidizes the sample and separates ^3H_2O and $^{14}CO_2$ into separate scintillation vials for counting. For lipid analysis, another piece of heart (~50 mg) was used for lipid extraction and class separation using methods detailed in Ref. 19. Briefly, heart tissue was extracted in chloroform-methanol (2:1), and organic and aqueous phases were then separated. An aliquot of the aqueous phase was used to determine clearance of radioactivity into the aqueous fraction. Lipid class separation was performed using thin-layer chromatography with quantification of radioactivity in free fatty acid (FFA), TG, monoglyceride (MG), diglyceride (DG), phospholipid (PL), and cholesterol ester (CE) fractions.

Measurement of ^{3}H and ^{14}C activities. Sample ^{3}H and ^{14}C activities were measured using quench correction liquid scintillation spectrometry (Wallac 1409 counter; Wallac OY, Turku, Finland).

Calculations

Tracer data are expressed as fluxes using the general expression for the flux (R_{fx}) into a particular pathway product

$$R_{fx} = \frac{C_P \times m_{fx}}{\int_0^T C_f(t)dt}$$

where C_P is the buffer/plasma FFA (or glucose) concentration, m_{fx} is the radioactivity from the tracer that is cleared into pathway × (expressed per unit heart weight), c_f is the buffer/plasma concentration of tracer (expressed as radioactivity per unit volume), and T is the duration of cardiac exposure to buffer/plasma tracer. Given the satisfaction of certain conditions (discussed in Ref. 34), including transient tracer exposure, T sufficient, and assuming that the products are completely trapped, these values for [^{14}C]P should estimate genuine FFA fluxes. The values obtained for the [^{3}H]R-BrP and [^{14}C]2-DG data provide apparent FFA and glucose fluxes, respectively.

For ex vivo experiments, where tracer levels were effectively constant over the exposure period, the integral in the denominator of the above equation was calculated as $c_f \times T$. Table 2 defines the flux parameters used to describe the ex vivo results. For in vivo experiments previously conducted in rats, this integral has been assessed by measuring tracer concentrations at multiple time points (requiring rapid collection of numerous blood samples), performing curve fitting and analytic integration using the best fit parameters (34). The current continuous sample withdrawal method is theoretically more accurate and requires the analysis of only a single blood sample. For the calculation of R_f*, our index of cardiac FFA utilization obtained using the [^{3}H]R-BrP tracer, the integral in the denominator was calculated as $\bar{c}_B \times T$, where $\bar{c}_B$ is the average [^{3}H]R-BrP over the 12-min experiment, equal to the pooled sample activity at the end of the experiment. An analogous expression was used for the calculation of R_g', the index of cardiac glucose utilization, from the pooled plasma [^{14}C]2-DG activity.

Statistics

Linear regression analysis of individual data points was performed using the program SPSS (SPSS, Chicago, IL). Group means were compared using the following a priori contrasts, which were tested on the basis of *F*-tests using SPSS: *db/db* fasted vs. control fasted; *db/db*-glucose vs. control-glucose; *db/db* fasted vs. *db/db*-glucose;

Table 2. *Flux parameters*

Parameter	Assesses	Obtained From
R_{aq}	FFA oxidation (tissue)	Aqueous phase ^{14}C activity in heart
$R_{fox(CO_2)}$	FFA oxidation (CO_2)	Perfusate + hyamine trap $^{14}CO_2$
R_{fox}	FFA oxidation (total)	$R_{fox(CO_2)} + R_{aq}$
R_{fs}	FFA storage	Organic phase ^{14}C activity in heart
R_{ftg}	FFA storage as TG	Triglyceride fraction ^{14}C activity in heart
R_f	FFA uptake	$R_{fox} + R_{fs}$
R_f*	^{3}H-R-BrP uptake	Total ^{3}H activity − [^{3}H]R-BrP in heart

[^{3}H]R-BrP, (R)-2-[9,10-^{3}H]bromopalmitate; TG, triglyceride.

and control-glucose vs. control-fasted. Group results are presented as means ± SE. $P < 0.05$ was considered statistically significant.

RESULTS

Ex Vivo Study of Perfused Hearts from Control Mice: Assessment of Cardiac FFA Metabolism with [^{3}H]R-BrP

Conditions utilized for individual perfusion experiments (Table 1) were varied with the intention of generating a range in FFA metabolism to correlate [^{3}H]R-BrP with [^{14}C]P uptake and metabolism. Indeed, the flux of [^{14}C]P into $^{14}CO_2$ released from hearts [represented by $R_{fox(CO_2)}$, *x*-axis; Fig. 2*A*] varied across a 15-fold range, from a low level in hearts exposed to insulin to a relatively high level in the heart without insulin and performing extra work. As shown in Fig. 2*A*, $R_{fox(CO_2)}$ was highly correlated with the flux of perfusate [^{14}C]P into the aqueous extract of hearts (R_{aq}, *y*-axis; Fig. 2*A*), which probably represents [^{14}C]P oxidation (or mitochondrial [^{14}C]P entry) not resulting in $^{14}CO_2$ release from the heart. Thus ^{14}C label in the aqueous extract of the heart probably includes ^{14}C-labeled amino acids [resulting from TCA exchange reactions (41)] together with [^{14}C]TCA intermediates and short-chain acylcarnitines (49). Because of the high likelihood that R_{aq} does reflect a quantitatively important component of [^{14}C]P oxidation, total [^{14}C]P flux into oxidation (R_{fox}) was estimated as the sum of R_{aq} and $R_{fox(CO_2)}$ (Table 2).

Results for the component of FFA uptake directed into nonoxidative metabolism are illustrated in Fig. 2*B*. R_{fs}, on the *x*-axis, represents incorporation into all lipid classes (TG + MG + DG + PL + CE), and R_{ftg}, on the *y*-axis, represents incorporation into TG only. Although the nonoxidative disposal had a similar order of magnitude compared with oxidative disposal (Fig. 2*B* *x*-axis; compare Fig. 2*A* *x*-axis), a relatively narrower range of nonoxidative FFA metabolism resulted from the different perfusion conditions. Thus R_{fs} varied over approximately a twofold range only. Among the various lipid classes, TG was by far the major fate of FFA taken up in all perfused hearts, with R_{ftg} (*y*-axis, Fig. 2*B*) accounting for an average of 87% of R_{fs}. Results for other lipid classes (MG, DG, PL, and CE) are not presented due to their minor contribution to R_{fs}.

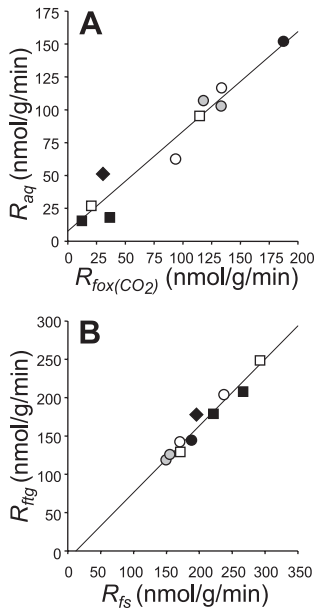

Fig. 2. Metabolic fate of buffer palmitate taken up by perfused mouse heart. *A*: relationship between the 2 putative components of oxidative disposal of buffer FFA into perfused mouse hearts. R_{aq} is obtained from clearance of [^{14}C]P into aqueous soluble, cardiac tissue-retained ^{14}C activity. $R_{fox(CO_2)}$ represents conversion of [^{14}C]P into $^{14}CO_2$. Line represents the linear regression equation $y = 7.9 + 0.76 \cdot x$, $r^2 = 0.94$. *B*: nonoxidative disposal of buffer FFA. R_{fs} represents flux of [^{14}C]P into all lipid classes in the heart. R_{ftg} is that component of R_{fs} directed into triglyceride (TG) synthesis. Line represents the linear regression equation $y = -10.9 + 0.87 \cdot x$, $r^2 = 0.95$. Perfusion conditions were varied as defined in Table 1: LoGluHiWork (●), LoGlu (gray circles), Norm (○), LoIns (□), HiIns (■), and PoorFunct (◆).

Figure 3 shows the main results of the ex vivo perfused heart study: the relationship between uptake of [^{3}H]R-BrP (R_f*) and the uptake and metabolism of [^{14}C]P. R_f* was calculated from the sum of all metabolic products of [^{3}H]R-BrP in the heart, i.e., total ^{3}H activity minus unmetabolized [^{3}H]R-BrP.

Previously, we considered [^{3}H]R-BrP uptake to reflect total FFA uptake (33), independently of metabolic fate, but the current results do not support this view in the heart. Although there was a strong association between [^{3}H]R-BrP flux parameter (R_f^*) and the rate of FA oxidation (R_{fox}) ($r^2 = 0.94$, $P < 0.0001$; Fig. 3*B*) there was no correlation with the storage component R_{fs} ($r^2 = 0.05$, $P = 0.52$; Fig. 3*C*). Because fluxes into oxidation and storage pathways were of similar magnitude, these results indicate that R_f^* much more closely reflects FFA oxidation than storage.

A significant correlation was observed between R_f^* and total FFA uptake (R_f), but this would be expected, since R_{fox} is the major component of R_f. However, the relationship between R_f^* and R_f was weaker (Fig. 3*A*, $r^2 = 0.79$) than that between R_f^* and R_{fox} (Fig. 3*B*, $r^2 = 0.94$), consistent with the notion that, in the heart, [^{3}H]R-BrP traces FFA oxidation rather than total uptake.

We also investigated a multiple regression model for R_f^* with R_{fox} and R_{fs} as independent variables. The model r^2 essentially did not improve over that obtained with the simple regression of R_f^* against R_{fox} ($r^2 = 0.94$). Unlike R_{fox} ($P < 0.0001$), neither R_{fs} (P = 0.64) nor the interaction term ($P = 0.85$) contributed significantly to the prediction of R_{fs} in the multiple regression model.

On the basis of all the results above, we conclude that variation in the R_f^* parameter primarily reflects variation in oxidative metabolism in the mouse heart; i.e., R_f^* provides an index of R_{fox}.

In Vivo Study 1: Cardiac FFA Metabolism in Control Mice In Vivo

By analogy with the ex vivo study, conditions were varied between individual control mice studied (Table 3) with the intention of producing a wide range in cardiac FFA oxidation. Figure 4*A* plots the individual R_f* vs. R_{fs} results. Whereas R_{fs} varied over a less than threefold range, R_f* varied across an ~20-fold range from low levels in the hyperglycemic/hyperinsulinemic mice to high levels during normoglycemia/fasting insulin levels and chronotropic/inotropic stimulation with dobutamine (evidenced by the elevated CWI; Table 3). Absolute rates of FFA oxidation (R_{fox}) estimated by extrapolating the linear regression equation obtained from the ex vivo study ($R_f^* = 17.6 + 0.29 \cdot R_{fox}$) ranged from 3 to 1,017

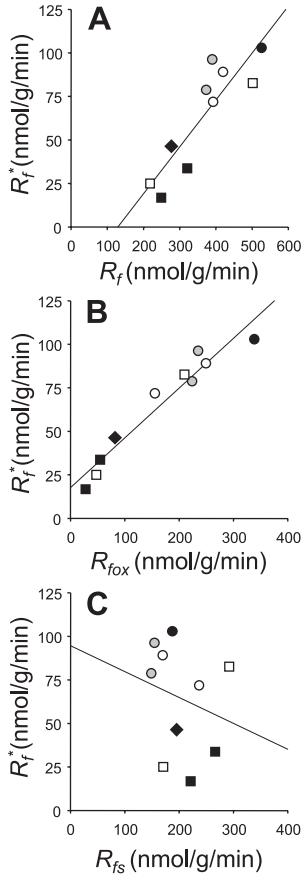

Fig. 3. Uptake of [^{3}H]R-BrP vs. native FFA uptake and metabolic fate in perfused mouse hearts. R_f^*, based on uptake of buffer [^{3}H]R-BrP, is plotted against R_f, uptake of buffer palmitate (*A*), based on oxidative + nonoxidative [^{14}C]P metabolism; R_{fox}, oxidation rate of buffer palmitate (*B*); and R_{fs}, flux of palmitate into nonoxidative (storage) metabolism (*C*). Perfusion conditions were varied as defined in Table 1: LoGluHiWork (●), LoGlu (gray circles), Norm (○), LoIns (□), HiIns (■), and PoorFunct (◆). Lines represent linear regression equations: $R_f^* = -34.9 + 0.27 \cdot R_f$, $r^2 = 0.79$ (*A*); $R_f^* = 17.6 + 0.29 \cdot R_{fox}$, $r^2 = 0.94$ (*B*); $R_f^* = 94.7 - 0.15 \cdot R_{fs}$, $r^2 = 0.05$ (*C*).

nmol·g^{-1}·min^{-1} in the hyperglycemic/hyperinsulinemic and dobutamine groups, respectively. It should be noted that the R_f* vs. R_{fs} pattern observed for the heart was atypical. Thus, although the major focus of this study was the heart, we actually examined various tissues, including diaphragm, hindlimb muscles, adipose tissue, and liver. In all of these tissues, a strong positive correlation was observed between R_f* and R_{fs}, as illustrated in Fig. 4*B* for diaphragm, in complete contrast to the pattern observed for heart (Fig. 4*B*).

Table 3. *Plasma glucose, FFA, and insulin concentrations and CWI in control mice used in in vivo study 2*

Condition	*n*	Glucose, mM	FFA, mM	Insulin, nM	CWI
Dobutamine	2	5.3	0.35	0.13	573
Fasted	2	5.1	0.36	0.08	339
Fed	1	6.8	0.19	1.10	270
Glucose infused	2	11.5	0.10	0.86	332

Results are means for n = 1–2 mice studied in each group. Cardiac work index (CWI) is the product of mean arterial pressure (MAP) and heart rate (HR) divided by heart weight (mmHg·bpm·mg^{-1}).

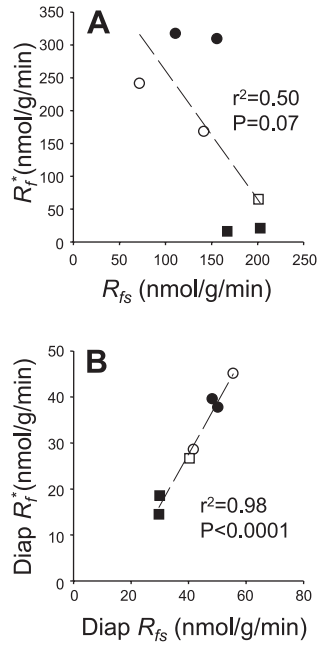

Fig. 4. In vivo tissue R_f* vs. R_{fs} in control mice. *A*: results for heart. *B*: results for diaphragm (Diap). Individual animals were subjected to different conditions: inotropic/chronotropic stimulation, applied in the fasting state, using constant iv dobutamine infusion (●), fasting state (○), fed state (□), and hyperglycemia/hyperinsulinemia achieved using iv glucose infusion (■).

To gauge the quantitative importance of R_{aq} in the in vivo situation, R_{aq} is plotted as a function of estimated R_{fox} (Fig. 5). For comparison, data from the ex vivo study are also included. The slope of the line relating R_{aq} to R_{fox} was much lower in vivo compared with ex vivo (0.022 ± 0.013 vs. 0.44 ± 0.02, respectively). This clearly suggests that, in contrast to the ex vivo situation, R_{aq} is a minor fate in vivo.

In Vivo Study 2: Cardiac Metabolism in Diabetic and Nondiabetic Mice

Body weights, heart weights, and cardiovascular parameters in the four groups of 12-wk-old mice studied are presented in

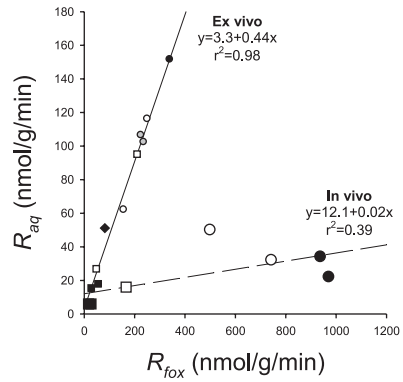

Fig. 5. Relationship between R_{aq} and estimated R_{fox} in control hearts. Small symbols represent data obtained from isolated perfused hearts (different symbols represent different study conditions as defined in the legend to Fig. 2). Solid line represents the linear regression equation for this ex vivo data. Large symbols represent data obtained from in vivo experiments in control mice (symbols defined as in Fig. 4). Broken line represents the regression equation for this in vivo data.

Table 4. *Body weight, heart weight, MAP, HR, and CWI in control (db/+) and diabetic (db/db) mice in the fasting state and during iv glucose infusion*

	db/+		*db/db*	
	Fasted	Glucose	Fasted	Glucose
Body weight, g	27.7±0.3	25.6±0.8	46.6±1.1†	44.5±1.2†
Heart weight, mg	105±3	102±4	107±4	98±3
MAP, mmHg	96±2	97±3	103±4	104±4
HR, beats/min	425±11	433±9	452±9	450±15
CWI	397±12	404±22	438±14	455±14†

CWI is the product of MAP and HR divided by heart weight (mmHg·bpm·mg^{-1}). Results are expressed as means ± SE; n = 6–7. †P < 0.05 vs. respective *db/+* mice (fasted or glucose).

Table 4. As expected, the diabetic (*db/db*) animals had greater body weights than their age-matched nondiabetic (*db/+*) controls. Despite this large difference in body mass, heart weight was similar in the *db/db* compared with control mice. Glucose infusion had no apparent effect on the cardiovascular parameters, mean arterial blood pressure (MAP), or heart rate (HR) in either the control or the *db/db* mice. CWI, the product of HR and MAP divided by heart weight, was calculated as an index of cardiac work. A subtle (nonsignificant) tendency for both mean HR and MAP to be higher in the *db/db* groups resulted in a modestly elevated CWI in the diabetic compared with the nondiabetic mice.

Under the basal fasting condition, *db/db* mice exhibited hyperglycemia with a marked increase in plasma insulin (Table 5), consistent with insulin resistance in this type 2 diabetic model. Other diabetic parameters in *db/db* mice included an elevation in ketone bodies (β-HBA), although plasma TG levels were not elevated.

The main results of the study, indexes of in vivo rates of FFA and glucose utilization, are presented in Fig. 6, together with the major determinants of these fuel utilization rates: *1*) circulating fuel levels (glucose and FFA) and *2*) the local ability of cardiac tissue to take up and utilize these fuels, tissue clearance, K_f* (= R_f*/plasma FFA concentration) and K_g' (= R_g'/plasma glucose concentration). Plasma FFA and glucose levels can influence cardiac FFA and glucose utilization via simple mass action. In the basal fasting state, plasma FFA and glucose levels were much higher in the *db/db* than in control mice, by 138 and 409%, respectively (P < 0.05). To assess metabolic flexibility, glucose infusion (of substantial but physiological magnitude) was performed to create a pseudo-fed state to contrast with the basal fasting situation. In the nondiabetic animals, glucose infusion induced a clear metabolic response, including increased plasma glucose level (by 8.6 mM, P < 0.05), increased insulin secretion (Table 5), and suppression of plasma FFA level (Fig. 6). In contrast, a blunted response was apparent in the diabetic animals. Glucose infusion raised mean glucose levels in the glucose infused *db/db* group compared with the fasted *db/db* group by 7.6 mM (similar in magnitude to the glucose increment seen in the nondiabetic animals), although the interanimal variability in this parameter prevented this group difference from achieving statistical significance. There was no evidence of an increase in insulin secretion in response to glucose infusion (Table 5) and no significant effect on plasma FFA level in the *db/db* group (Fig. 6).

Cardiac utilization of plasma substrate is not just a function of the circulating substrate level but is also determined by local factors including the influence of metabolic mechanisms that control the substrate's uptake and sequestration. R_f* and K_f* data are presented in Fig. 6. In the basal fasting state, despite the high circulating levels of FFA in the *db/db* mice, R_f* in these animals was actually substantially lower than in the control mice. This resulted from a much lower K_f* in the diabetic hearts. In the control animals, glucose infusion acutely suppressed R_f* (−75%) via systemic and local cardiac effects; circulating FFA levels were lowered and K_f* was reduced (−45%, P < 0.05), respectively. This reduction in K_f* is particularly significant and demonstrates the operation of a powerful metabolic mechanism controlling the uptake and utilization of available FFA in the hearts of these nondiabetic animals. By contrast, in the *db/db* animals, glucose infusion had no apparent effect on either R_f* or K_f*. In the glucose-infused state, therefore, R_f* was higher in the *db/db* than in the control mice.

R_g' indexes the rate of plasma glucose uptake and utilization (hexokinase-catalyzed phosphorylation), whereas K_g' indexes the heart's ability to take up and utilize available plasma glucose. These data are presented in Fig. 6, *bottom*. In the basal fasting state, despite profound hyperglycemia (and hyperinsulinemia; Table 5), R_g' in *db/db* mice was very similar to that in normoglycemic control mice. This was due to a markedly lower K_g' in the diabetic animals. In the control animals, glucose infusion raised R_g' (by 60%) but not K_g', probably the net result of opposing influences of changes in plasma glucose and insulin levels induced by the glucose infusion. Thus, in isolation, the observed increase in insulin level in control mice (Table 5) would be expected to increase K_g', whereas on its own the increase in plasma glucose level would be expected to decrease K_g'. In the *db/db* animals, there was no apparent alteration in either R_g' or K_g' in response to glucose infusion.

Plasma glucose and FFA are not the only circulating fuels available to the heart; lactate and ketone bodies are cardiac substrates along with the FFA derived from hydrolysis of plasma TG. Plasma TG was low and similar across all four groups of mice. In the fasting state, diabetic mice had elevated levels of lactate and β-HBA compared with the nondiabetic animals. In control mice, glucose infusion raised plasma lactate concentration (+63%) and suppressed β-HBA levels (−47%). No effects of glucose infusion were apparent on either lactate or ketone body levels in the *db/db* mice.

Table 5. *Plasma measurements in control (db/+) and diabetic (db/db) mice in the fasting state and during an intravenous glucose infusion*

	db/+		*db/db*	
	Fasted	Glucose	Fasted	Glucose
Insulin, nM	0.12±0.07	0.74±0.09*	3.66±0.63†	3.09±0.56†
TG, mM	0.34±0.03	0.41±0.08	0.43±0.04	0.52±0.05
Lactate, mM	1.7±0.3	2.8±0.2*	3.1±0.3†	3.7±0.3†
β-HBA, μM	75±14	40±4*	191±34†	167±22†

Results are expressed as means ± SE; n = 6–7. β-HBA, β-hydroxybutyrate. *P < 0.05 vs. fasted state; †P < 0.05 vs. respective *db/+* mice (fasted or glucose).

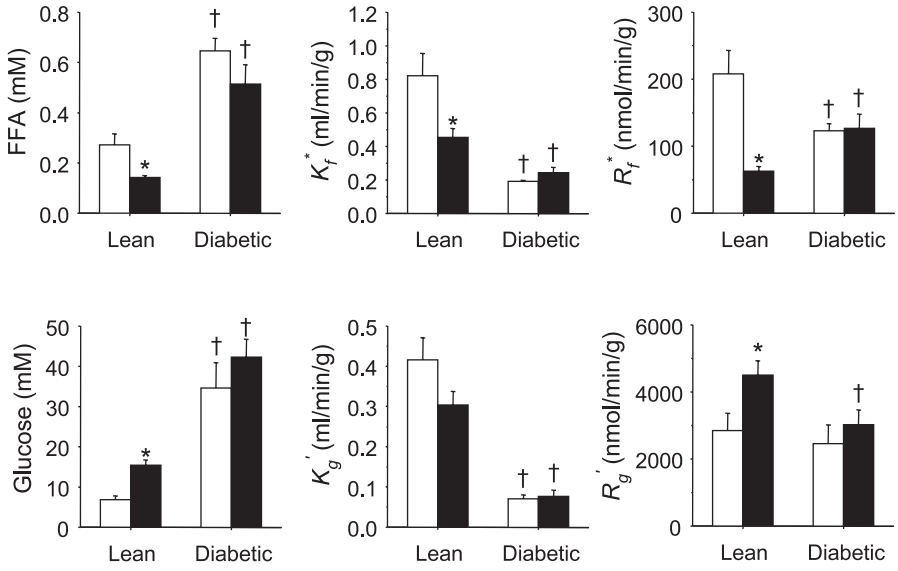

Fig. 6. Cardiac utilization of plasma FFA and glucose in nondiabetic control and diabetic (*db/db*) mice in the fasting state (open bars) and during iv glucose infusion (filled bars). Results are expressed as means ± SE; $n = 6–7$. *$P < 0.05$ vs. fasted state, †$P < 0.05$ vs. respective *db/+* mice (fasted or glucose infused).

DISCUSSION

Cardiac metabolism of *db/db* mice, an animal model of type 2 diabetes, has been largely studied ex vivo (1, 3, 7) using isolated hearts perfused with fixed concentrations of glucose and palmitate in the absence of insulin and other substrates for oxidative metabolism (e.g., ketone bodies and lactate) and at standardized levels of cardiac pre- and afterload conditions. These studies have revealed an altered metabolic phenotype; FFA utilization was elevated, whereas glucose utilization was reduced in isolated perfused working *db/db* hearts (1, 3, 5). It has been proposed that this altered metabolic phenotype could be a causative factor in the contractile dysfunction observed in *db/db* hearts (5, 34). Therefore, it is important to establish whether a similar metabolic phenotype with increased FFA utilization is also observed with *db/db* mice in vivo.

In the present study, metabolism of plasma glucose and FFA by hearts of control and *db/db* mice has, for the first time, been studied in vivo. To achieve this, we first adapted our existing tracer methods originally developed for use in rats (25, 34) to the mouse, yielding reliable tracer kinetic data without gross disturbance to systemic cardiovascular function in this small animal (~1/10th the size of a rat). [^{3}H]R-BrP is used to obtain R_f^*, an index of the rate of plasma FFA utilization, and [^{14}C]2-DG to obtain R_g', an index of the rate of plasma glucose utilization. In addition, because no details were available concerning the evaluation of cardiac FFA metabolism with [^{3}H]R-BrP in the mouse heart, studies of isolated control mouse hearts were made to investigate the quantitative nature of the relationship between R_f* and palmitate uptake and metabolism. R_f* was tightly correlated with the rate of palmitate oxidation (R_{fox}), with a proportionality constant equal to 0.29 (Fig. 3*B*). To provide qualitative confirmation that R_f* represents a valid index of R_{fox} in vivo, a group of control mice were studied in which physiological conditions were varied between individual animals with the intention of creating a wide range in cardiac FFA oxidation rates. Indeed, this succeeded in producing an ~20-fold range in R_f*, with the pattern of results consistent with physiological expectations (Fig. 4*A*), i.e., hyperinsulinemia/hyperglycemia < fasting state < elevated cardiac work.

Our data indicate that the diabetic heart exhibits profound metabolic inflexibility with the total failure of glucose loading to alter either R_g' or R_f^* (Fig. 6). Furthermore, whole body insulin resistance together with pancreatic β-cell failure in these animals probably mean that insulin secretion is maximal even under basal fasting conditions. This would explain the apparent failure of the glucose challenge to further stimulate insulin secretion (Table 5). The current experimental design does not directly address the issue of insulin sensitivity in the heart. However, the observation that R_g' could be stimulated to a higher level in the *db/+* animals, despite their much lower insulin levels compared with the *db/db* animals, implies substantial cardiac insulin resistance in the diabetic heart. This indirect evidence is compatible with the observation of reduced insulin-stimulated glucose uptake in cardiomyocytes isolated from *db/db* mice (8). The glucose metabolic insulin resistance may be dependent on the elevated plasma FFA availability in the diabetic state. Thus in nonhypertensive patients with type 2 diabetes, cardiac glucose utilization was reduced during hyperinsulinemia if circulating fatty acid levels were elevated at the time of assessment of glucose utilization (31, 50) (as they are in the *db/db* animals) but not if fatty acid levels were normal (47). Moreover, enhancement of insulin-stimulated cardiac glucose utilization by rosiglitazone treatment of patients with type 2 diabetes has been associated with improved insulin-mediated suppression of plasma FFA levels (18).

By contrast with the *db/db* heart, the current data imply that cardiac metabolism in the nondiabetic mice (with the same genetic background as the *db/db* mice) exhibits a high degree of metabolic flexibility, with alteration in fuel utilization involving both systemic and local influences. Thus suppression of R_f^* by the glucose infusion resulted from both a reduction in circulating FFA levels (presumably a consequence of a normal level of insulin action in adipose tissue to restrain FFA mobilization) and an apparent local suppression in the FFA utilization of available FFA in the heart tissue itself (Fig. 6). This local mechanism is deduced from the large reduction in the K_f* parameter. The current results from the *db/+* mice are compatible with our previous findings in healthy Wistar rats (14)

where physiological hyperinsulinemia induced a similar relative suppression of K_f^*. The K_f^*-lowering effect is particularly significant considering that plasma FFA lowering per se would be expected to actually increase K_f* via reduced competition of the tracer with native FFA for transporters and enzymatic activation. A likely mechanistic basis for this local inhibition of FFA utilization is the so-called "reverse glucose-fatty acid cycle." That is, the increase in glucose utilization in response to glucose infusion resulted in increased cytosolic malonyl-CoA levels, which in turn inhibited FFA entry into mitochondria (7). Coincident with the glucose load-induced suppression of R_f^* by the *db/+* heart, R_g' increased, an expected consequence of the observed elevations in plasma glucose and insulin levels. Thus our data indicate that the healthy mouse heart exhibits a substantial shift toward a greater reliance on plasma glucose utilization and a reduced reliance on plasma FFA oxidation in the transition from the basal fasting state induced by the glucose challenge.

On the basis of the present data, metabolic inflexibility rather than a fixed alteration in fatty acid (vs. glucose) utilization seems to best define the metabolic defect in the db/db mouse heart. Thus, despite the profound disturbances in systemic metabolism in the diabetic animals, the R_f^* data (Fig. 6) indicate that the average level of cardiac FFA oxidation is comparable to that of the normal animals. This is evidenced by the fact that R_f^* averaged across the basal fasting and glucose-infused (pseudo-fed) states was very similar in the *db/db* (125 $nmol \cdot g^{-1} \cdot min^{-1}$) and *db/+* (135 $nmol \cdot g^{-1} \cdot min^{-1}$) animals. Neither was the apparent magnitude of glucose utilization profoundly influenced by diabetes; averaged over the two states, R_g' in *db/db* hearts was only moderately less (by 16%) than in the control animals.

The fact that FFA utilization in the diabetic animals was apparently not elevated in the fasting state, despite their high plasma FFA levels, resulted from an apparent reduction in the capacity of cardiac tissue to clear available FFA, reflected in the lower values of K_f^* (Fig. 6). This finding of reduced in vivo cardiac FFA clearance is consistent with the results of two earlier studies of diabetic rodents, based on reductions in the cardiac deposition of radioactivity following in vivo administration of β-methyl-*p*-iodophenylpentadecanoic acid tracer to KK-A^Y mice (36) and rats with chronic diabetes induced by streptozotocin (40). We have found one study in patients with type 2 diabetes with which to compare our results. Cardiac FFA utilization was studied after an overnight fast by using myocardial kinetics of a fatty acid analog, ^{123}I-labeled heptadecanoate (46). Although not statistically significant, the results were actually in qualitative agreement with the results of the present study, with patients having a tendency to have lower indexes of cardiac FFA uptake and oxidation than the control subjects.

There are probably several reasons for the apparent reduction in FFA clearance in the diabetic heart, including substrate competition, but a major factor is likely related to cardiac lipid overloading. One striking manifestation of the diabetic condition in the *db/db* mouse heart is a tremendous accumulation of intramyocellular lipid droplets (15). This situation must result from a previous mismatch between fatty acid uptake and oxidation. The accumulation of lipid intermediates would, however, via feedback regulation and increased competition, be expected to eventually result in a decrease in plasma FFA clearance and a new steady-state situation where uptake and oxidation are matched (or nearly matched) in the presence of higher lipid intermediate levels. An important point that emerges from this is that a condition of lipid overload can exist in the absence of an elevation in lipid utilization.

Our previous observation that major metabolic inflexibility prevails in the cardiac tissue of obese Zucker rats (35) that are nondiabetic suggests that this condition evolves early in the pathogenesis of diabetes. We propose that metabolic inflexibility is a consequence of intracellular accumulation of metabolic products of fatty acids due to systemic hyperlipidemia, ultimately a result of obesity and adipose tissue insulin resistance. Thus accumulation of storage products of fatty acids, notably TG, in the myocardial cells tends to force continuous lipid utilization, thereby interfering with normal glucose-fatty acid fuel switching. Additionally, accumulation of other fatty acid intermediates, especially DGs and ceramides, has been implicated in the induction of glucose metabolic insulin resistance, cellular damage, and even apoptosis (5, 52).

The apparent similarity in "average" cardiac fuel utilization between the diabetic and control animals in vivo is not evident in isolated hearts perfused with fixed concentrations of glucose and FFA. In the ex vivo situation, *db/db* hearts exhibit reduced glucose utilization (decreased rates of glycolysis and glucose oxidation) with corresponding increased rates of FFA oxidation (1, 3, 7). This pattern of fuel use is also compatible with the upregulation of genes involved in fatty acid oxidation in cardiac tissue of *db/db* mice (6). Differences in the metabolic environments of the ex vivo and in vivo settings may play an important role in the discrepancy between the ex vivo and in vivo results. Lactate and ketone bodies, absent from the ex vivo perfusates, are both elevated in the *db/db* animals and have been shown to inhibit FFA oxidation (42, 43) as well as glucose metabolism. The extent of inhibition of glucose oxidation is greater than inhibition of glycolysis and much greater than inhibition of glucose transport/phosphorylation (12). The extreme hyperinsulinemia in the diabetic animals in vivo could also be the basis of divergence of the in vivo and ex vivo results.

Results of the present study have important implications for the interpretation of [^{3}H]R-BrP uptake by the heart. In particular, our original assumption that R_f^* is equally dependent on oxidative and nonoxidative disposal of FFA (34) is clearly not true. Instead, R_f^* appears to very selectively assess FFA oxidation in the murine myocardium but probably not in other tissues. Thus, in all noncardiac tissues examined, including diaphragm, hindlimb muscle, and liver, a strong positive correlation was observed between R_f* and R_{fs} (as illustrated in Fig. 4*B* for diaphragm), in contrast to the pattern observed for the heart (Fig. 4*A*). This suggests that, in noncardiac tissues, [^{3}H]R-BrP uptake is responsive to changes in FA storage as well as changes in oxidation (34) and most likely is an index of total FA uptake. The dependence of R_f^* on FA oxidation alone in the mouse would appear to be limited to heart muscle.

There are several possible explanations for the differential sensitivity of [^{3}H]R-BrP to oxidative vs. storage metabolism in the heart. First, one or more of the transfer or transformation processes committing FFA to these alternative pathways could have a differential selectivity for [^{3}H]R-BrP compared with [^{14}C]P. For example, the metabolic sequestration step for oxidation and storage in the heart may be mediated by different

isoforms of long-chain acyl-CoA synthetases (ACS), as is the case in liver where ACS1 and ACS5 have been suggested to sequester FFA for acylglyceride synthesis and mitochondrial oxidation, respectively (11, 23). A differential selectivity of the putative enzyme directing FFA to mitochondrial oxidation for analog vs. native FFA could, in turn, give rise to the observed difference in sensitivity of [^{3}H]R-BrP. Another possible explanation for the apparent insensitivity of [^{3}H]R-BrP to storage metabolism in the heart is that ^{3}H label entering the storage pathway is rapidly lost from this tissue, whereas that directed into oxidative metabolism is effectively trapped, e.g., as part of a ternary complex together with carnitine and carnitine palmitoyltransferase (9, 29). Future studies will, hopefully, define the metabolic fate of [^{3}H]R-BrP.

The [^{14}C]P taken up by the ex vivo heart had three major fates: *1*) [^{14}C]TG, *2*) $^{14}CO_2$, and *3*) ^{14}C product/s that partitioned into the aqueous fraction of the tissue extract. The ^{14}C activity of the latter product/s was both very closely correlated (with zero intercept) and of similar magnitude to the ^{14}C activity liberated from the heart as $^{14}CO_2$ (Fig. 2*A*). On the basis of these observations, we concluded that this label most probably resulted from [^{14}C]palmitate entering β-oxidation. FFA oxidation was therefore estimated on the basis of the sum of $^{14}CO_2$ released from the heart and the ^{14}C activity in the aqueous fraction of the isolated heart. The identity of the aqueous ^{14}C product is unknown, but [^{14}C]bicarbonate was eliminated as a possible candidate by our analysis. Evidence, consistent with our own, that a substantial fraction of total [^{14}C]palmitate oxidation does not result in $^{14}CO_2$ production has been obtained in various in vitro systems, e.g., Ref. 49. Although significant label fixation can occur in vivo (41), our own data in the mouse heart indicates that the magnitude of this process is much greater in the ex vivo situation than in the in vivo one. This might be the result of accumulation of acetyl-CoA, acetylcarnitine, and citric acid cycle intermediates in the ex vivo situation.

In conclusion, methods for assessment of plasma FFA and glucose metabolism in individual tissues in vivo have been optimized for use in mice. In the diabetic mice, a severely limited cardiac metabolic flexibility implies a virtually fixed utilization of plasma glucose and FFA across the postprandial and postabsorptive situations. An important consequence of the current findings is that characterization of cardiac metabolism in metabolically disturbed states, e.g., type 2 diabetes, needs to be performed with consideration to the large shifts in fuel utilization seen in different physiological states of the metabolically flexible healthy myocardium.

ACKNOWLEDGMENTS

We are grateful to Dr. Shalini Andersson (AstraZeneca) for developing and simplifying the method for enantiomeric purification of the (R)-2-[9,10-^{3}H]bromopalmitate tracer.

GRANTS

A. Edgley is supported by a National Health & Medical Research Council of Australia Industry Fellowship (Grant no. 237003). This study was supported in part by an operating grant (MT13227) awarded to D. L. Severson from the Canadian Institutes of Health Research. E. Aasum and T. Larsen acknowledge the support of the Norwegian Heart Foundation (Grant no. 6412).

REFERENCES

1. **Aasum E, Hafstad AD, Severson DL, and Larsen TS.** Age-dependent changes in metabolism, contractile function, and ischemic sensitivity in hearts from db/db mice. *Diabetes* 52: 434–441, 2003.
2. **Andersson S.** Synthesis, resolution and application of the enantiomers of 2-bromopalmitic acid in the evaluation of free fatty acid metabolism in vivo (Abstract). *International Symposium on Chirality, Parma, Italy*, 2005.
3. **Belke DD, Larsen TS, Gibbs EM, and Severson DL.** Altered metabolism causes cardiac dysfunction in perfused hearts from diabetic (*db/db*) mice. *Am J Physiol Endocrinol Metab* 279: E1104–E1113, 2000.
4. **Belke DD, Larsen TS, Lopaschuk GD, and Severson DL.** Glucose and fatty acid metabolism in the isolated working mouse heart. *Am J Physiol Regul Integr Comp Physiol* 277: R1210–R1217, 1999.
5. **Boden G.** Effects of free fatty acids (FFA) on glucose metabolism: significance for insulin resistance and type 2 diabetes. *Exp Clin Endocrinol Diabetes* 111: 121–124, 2003.
6. **Buchanan J, Mazumder PK, Hu P, Chakrabarti G, Roberts MW, Yun UJ, Cooksey RC, Litwin SE, and Abel ED.** Reduced cardiac efficiency and altered substrate metabolism precedes the onset of hyperglycemia and contractile dysfunction in two mouse models of insulin resistance and obesity. *Endocrinology* 146: 5341–5349, 2005.
7. **Carley AN and Severson DL.** Fatty acid metabolism is enhanced in type 2 diabetic hearts. *Biochim Biophys Acta* 1734: 112–126, 2005.
8. **Carroll R, Carley AN, Dyck JR, and Severson DL.** Metabolic effects of insulin on cardiomyocytes from control and diabetic *db/db* mouse hearts. *Am J Physiol Endocrinol Metab* 288: E900–E906, 2005.
9. **Chase JF and Tubbs PK.** Specific inhibition of mitochondrial fatty acid oxidation by 2-bromopalmitate and its coenzyme A and carnitine esters. *Biochem J* 129: 55–65, 1972.
10. **Coleman DL.** Diabetes-obesity syndromes in mice. *Diabetes* 31: 1–6, 1982.
11. **Coleman RA, Lewin TM, Van Horn CG, and Gonzalez-Baro MR.** Do long-chain acyl-CoA synthetases regulate fatty acid entry into synthetic versus degradative pathways? *J Nutr* 132: 2123–2126, 2002.
12. **Depre C, Rider MH, and Hue L.** Mechanisms of control of heart glycolysis. *Eur J Biochem* 258: 277–290, 1998.
13. **Fang ZY, Prins JB, and Marwick TH.** Diabetic cardiomyopathy: evidence, mechanisms, and therapeutic implications. *Endocr Rev* 25: 543–567, 2004.
14. **Furler SM, Cooney GJ, Hegarty BD, Lim-Fraser MY, Kraegen EW, and Oakes ND.** Local factors modulate tissue-specific NEFA utilization: assessment in rats using 3H-(R)-2-bromopalmitate. *Diabetes* 49: 1427–1433, 2000.
15. **Giacomelli F and Wiener J.** Primary myocardial disease in the diabetic mouse. An ultrastructural study. *Lab Invest* 40: 460–473, 1979.
16. **Goudriaan JR, Dahlmans VE, Teusink B, Ouwens DM, Febbraio M, Maassen JA, Romijn JA, Havekes LM, and Voshol PJ.** CD36 deficiency increases insulin sensitivity in muscle, but induces insulin resistance in the liver in mice. *J Lipid Res* 44: 2270–2277, 2003.
17. **Hagenfeldt L.** A gas chromatographic method for the determination of individual free fatty acids in plasma. *Clin Chim Acta* 13: 266–268, 1966.
18. **Hallsten K, Virtanen KA, Lonnqvist F, Janatuinen T, Turiceanu M, Ronnemaa T, Viikari J, Lehtimaki T, Knuuti J, and Nuutila P.** Enhancement of insulin-stimulated myocardial glucose uptake in patients with Type 2 diabetes treated with rosiglitazone. *Diabet Med* 21: 1280–1287, 2004.
19. **Hamilton RJ and Hamilton S.** *Lipid Analysis A Practical Approach*. Oxford, UK: Oxford Univ. Press, 1992.
20. **Harwood HJ.** Reactions of the hydrocarbon chain of fatty acids. *Chem Rev* 62: 102–103, 1962.
21. **Hasselbaink DM, Glatz JFC, Luiken J, Roemen THM, and van der Vusse GJ.** Ketone bodies disturb fatty acid handling in isolated cardiomyocytes derived from control and diabetic rats. *Biochem J* 371: 753–760, 2003.
22. **Hernanz D, Camps F, Guerro A, and Delgado A.** Synthesis and configurational assignment of (R) and (S)-2-bromohexadecanoic acids. *Tetrahedron Asymm* 6: 2291–2298, 1985.
23. **Kim JH, Lewin TM, and Coleman RA.** Expression and characterization of recombinant rat Acyl-CoA synthetases 1, 4, and 5. Selective inhibition by triacsin C and thiazolidinediones. *J Biol Chem* 276: 24667–24673, 2001.

24. **Kirchner G, Scollar MP, and Klibanov AM.** Resolution of racemic mixtures via lipase catalysis in organic solvents. *J Am Chem Soc* 107: 7072–7076, 1985.
25. **Kraegen EW, James DE, Jenkins AB, and Chisholm DJ.** Dose-response curves for in vivo insulin sensitivity in individual tissues in rats. *Am J Physiol Endocrinol Metab* 248: E353–E362, 1985.
26. **Leibel RL, Chung WK, and Chua SC Jr.** The molecular genetics of rodent single gene obesities. *J Biol Chem* 272: 31937–31940, 1997.
27. **Lloyd S, Brocks C, and Chatham JC.** Differential modulation of glucose, lactate, and pyruvate oxidation by insulin and dichloroacetate in the rat heart. *Am J Physiol Heart Circ Physiol* 285: H163–H172, 2003.
28. **Lorenz JN.** A practical guide to evaluating cardiovascular, renal, and pulmonary function in mice. *Am J Physiol Regul Integr Comp Physiol* 282: R1565–R1582, 2002.
29. **McGarry JD, Sen A, Esser V, Woeltje KF, Weis B, and Foster DW.** New insights into the mitochondrial carnitine palmitoyltransferase enzyme system. *Biochimie* 73: 77–84, 1991.
30. **Minami A, Iseki M, Kishi K, Wang M, Ogura M, Furukawa N, Hayashi S, Yamada M, Obata T, Takeshita Y, Nakaya Y, Bando Y, Izumi K, Moodie SA, Kajiura F, Matsumoto M, Takatsu K, Takaki S, and Ebina Y.** Increased insulin sensitivity and hypoinsulinemia in APS knockout mice. *Diabetes* 52: 2657–2665, 2003.
31. **Monti LD, Landoni C, Setola E, Galluccio E, Lucotti P, Sandoli EP, Origgi A, Lucignani G, Piatti P, and Fazio F.** Myocardial insulin resistance associated with chronic hypertriglyceridemia and increased FFA levels in type 2 diabetic patients. *Am J Physiol Heart Circ Physiol* 287: H1225–H1231, 2004.
32. **Neely JR, Rovetto MJ, and Oram JF.** Myocardial utilization of carbohydrate and lipids. *Prog Cardiovasc Dis* 15: 289–329, 1972.
33. **Oakes ND and Furler SM.** Evaluation of free fatty acid metabolism in vivo. *Ann NY Acad Sci* 967: 158–175, 2002.
34. **Oakes ND, Kjellstedt A, Forsberg GB, Clementz T, Camejo G, Furler SM, Kraegen EW, Olwegard-Halvarsson M, Jenkins AB, and Ljung B.** Development and initial evaluation of a novel method for assessing tissue-specific plasma free fatty acid utilization in vivo using (R)-2-bromopalmitate tracer. *J Lipid Res* 40: 1155–1169, 1999.
35. **Oakes ND, Kjellstedt A, Thalen PG, Wettesten M, Löfgren L, and Ljung B.** Tissue-specific effects of AZ 242, a novel PPARa/g agonist, on glucose and fatty acid metabolism in obese Zucker rats: an in vivo multi-tracer assessment (Abstract). *Diabetes* 50: 121, 2001.
36. **Oshima M, Higashi S, Kikuchi Y, Shirai T, Yokokawa T, Kaminaga T, Yasukochi H, and Furui S.** Myocardial fatty acid metabolism in diabetic mice with 125I-BMIPP. *Ann Nucl Med* 12: 133–137, 1998.
37. **Pacini G, Thomaseth K, and Ahren B.** Contribution to glucose tolerance of insulin-independent vs. insulin-dependent mechanisms in mice. *Am J Physiol Endocrinol Metab* 281: E693–E703, 2001.
38. **Severson DL.** Diabetic cardiomyopathy: recent evidence from mouse models of type 1 and type 2 diabetes. *Can J Physiol Pharmacol* 82: 813–823, 2004.
39. **Sharma S, Adrogue JV, Golfman L, Uray I, Lemm J, Youker K, Noon GP, Frazier OH, and Taegtmeyer H.** Intramyocardial lipid accumulation in the failing human heart resembles the lipotoxic rat heart. *FASEB J* 18: 1692–1700, 2004.
40. **Shinmura K, Tani M, Suganuma Y, Hasegawa H, Hayashi Y, Guo XD, and Nakamura Y.** Myocardial uptake of iodine-125-labeled 15-(p-iodophenyl)-3-(R,S)-methyl pentadecanoic acid is decreased in chronic diabetic rats with changes in subcellular distribution. *Jpn Circ J* 62: 364–370, 1998.
41. **Sidossis LS, Coggan AR, Gastaldelli A, and Wolfe RR.** Pathway of free fatty acid oxidation in human subjects. Implications for tracer studies. *J Clin Invest* 95: 278–284, 1995.
42. **Spitzer JJ.** Effect of lactate infusion on canine myocardial free fatty acid metabolism in vivo. *Am J Physiol* 226: 213–217, 1974.
43. **Stanley WC, Meadows SR, Kivilo KM, Roth BA, and Lopaschuk GD.** β-Hydroxybutyrate inhibits myocardial fatty acid oxidation in vivo independent of changes in malonyl-CoA content. *Am J Physiol Heart Circ Physiol* 285: H1626–H1631, 2003.
44. **Storlien L, Oakes ND, and Kelley DE.** Metabolic flexibility. *Proc Nutr Soc* 63: 363–368, 2004.
45. **Taegtmeyer H, McNulty P, and Young ME.** Adaptation and maladaptation of the heart in diabetes. Part I: general concepts. *Circulation* 105: 1727–1733, 2002.
46. **Turpeinen AK, Kuikka JT, Vanninen E, and Uusitupa MI.** Abnormal myocardial kinetics of 123I-heptadecanoic acid in subjects with impaired glucose tolerance. *Diabetologia* 40: 541–549, 1997.
47. **Utriainen T, Takala T, Luotolahti M, Ronnemaa T, Laine H, Ruotsalainen U, Haaparanta M, Nuutila P, and Yki-Jarvinen H.** Insulin resistance characterizes glucose uptake in skeletal muscle but not in the heart in NIDDM. *Diabetologia* 41: 555–559, 1998.
48. **van der Vusse GJ, Glatz JF, Stam HC, and Reneman RS.** Fatty acid homeostasis in the normoxic and ischemic heart. *Physiol Rev* 72: 881–940, 1992.
49. **Veerkamp JH, van Moerkerk TB, Glatz JF, Zuurveld JG, Jacobs AE, and Wagenmakers AJ.** 14CO2 production is no adequate measure of [14C]fatty acid oxidation. *Biochem Med Metab Biol* 35: 248–259, 1986.
50. **Yokoyama I, Ohtake T, Momomura S, Yonekura K, Yamada N, Nishikawa J, Sasaki Y, and Omata M.** Organ-specific insulin resistance in patients with noninsulin-dependent diabetes mellitus and hypertension. *J Nucl Med* 39: 884–889, 1998.
51. **Young ME, McNulty P, and Taegtmeyer H.** Adaptation and maladaptation of the heart in diabetes. Part II: potential mechanisms. *Circulation* 105: 1861–1870, 2002.
52. **Zhou YT, Grayburn P, Karim A, Shimabukuro M, Higa M, Baetens D, Orci L, and Unger RH.** Lipotoxic heart disease in obese rats: implications for human obesity. *Proc Natl Acad Sci USA* 97: 1784–1789, 2000.